Available online at www.sciencedirect.com
SCIENCE DIRECT®
Journal of Nuclear Materials 324 (2004) 177–182
journal of nuclear materials
www.elsevier.com/locate/jnucmat

Oxidation behaviour of uranium in the internally gelated urania–ceria solid solutions – XRD and XPS studies

K. Suresh Kumar [a,*], T. Mathews [b], H.P. Nawada [c], N.P. Bhat [b]

[a] Kalpakkam Reprocessing Plant, Bhabha Atomic Research Centre (Facilities), Kalpakkam, Tamil Nadu 603 102, India
[b] Thermodynamics and Kinetics Division, Materials Characterization Group, Indira Gandhi Centre for Atomic Research, Kalpakkam, Tamil Nadu 603 102, India
[c] Nuclear Fuel Cycle and Materials Section, Division of Nuclear Fuel Cycle and Waste Technology, Department of Nuclear Energy, IAEA, P.O. Box 100, Wagramer Strasse 5, A-1400, Vienna, Austria

Received 8 August 2003; accepted 30 September 2003

Abstract

Single-phase UO_2–CeO_2 solid solutions were synthesized through an internal gelation route followed by gel decomposition at 600 °C in Ar laden with moisture and sintering at 1100 °C for 24 h in an atmosphere of Ar + 2% H_2. The sintered oxides were oxidized by heating in air at 600 °C for 24 h. The oxidation behaviour of U in the oxidized samples with different Ce contents were investigated using oxygen-to-metal ratio (O/M), X-ray diffraction (XRD) and X-ray photoelectron spectroscopy (XPS) analyses. The oxidized sample with Ce contents less than 70 mol% was found to be a mixture of orthorhombic and cubic phases and that with above 70 mol% Ce was found to be single-phase cubic. The valency of U in the oxidized samples computed from the O/M results was compared with the U $4f_{7/2}$ peak positions obtained from XPS.

1. Introduction

Urania–plutonia (UO_2–PuO_2) mixed oxide (MOX) fuel provides a means of burning weapon grade Pu in reactors for the generation of electricity. Diversion resistant reprocessing [1] gives a vent for the utilization of MOX fuel in reactors. There are various types of MOX fuel, with difference in the level of Pu introduced, typically ≈5% for thermal reactors, and 20–30% for fast reactors [2]. The stepwise oxidation of UO_2 in air to U_3O_8 has been extensively studied for about 40 years [3–8], because of its relevance to the dry storage and ultimate disposal of spent fuel [9–13]. A detailed review on the oxidation behaviour of U in uranium dioxide and the parameters which affect the rate of oxidation were discussed by MacEachern and Taylor [14]. The effect of dopants on the rate of oxidation of UO_2 has been studied [15,16] to gain insight into the different reactivities of UO_2 and spent fuel. Thomas et al. [17] found that UO_2 doped with 4–8% gadolinia oxidized at around 450 °C to a cubic phase resembling U_4O_9 and at around 575 °C to U_3O_8. A similar behaviour was observed during the oxidation of light water reactor spent fuel. In contrast, urania–niobia with a low dopant content of 0.4% NbO_2 was oxidized to U_3O_7 at around 400 °C which in turn oxidized to U_3O_8 at around 525 °C. A comparison of the oxidation behaviour of UO_2 and UO_2-based simulated high burn-up fuels was reported by Choi et al. [18]. They have observed that a high burn-up fuel is likely to be more resistant to U_3O_8 formation than the low burn-up fuel. Various authors [19–31] have carried out extensive studies on the oxidation behaviour of U in UO_2 and its mixed oxides by using X-ray photoelectron spectroscopy (XPS) and X-ray diffraction (XRD) techniques.

By employing O/M analysis, Nawada et al. [32] studied the valency of U in the oxidized products of various compositions of urania–ceria mixed oxides at

* Corresponding author. Tel.: +91-4114 280 224; fax: +91-4114 280 256.
E-mail address: ksuresh@igcar.ernet.in (K. Suresh Kumar).

0022-3115/$ - see front matter © 2003 Elsevier B.V. All rights reserved.
doi:10.1016/j.jnucmat.2003.09.014

different temperatures. Even though sufficient literature is available on the oxidation behaviour of U in UO_2, no reliable study is reported on the mixed oxides of U with Pu or Ce prepared through the soft chemistry routes. In the present study ceria (CeO_2) is used to simulate plutonia (PuO_2) in the MOX fuel [32–34] and an attempt is made to understand the oxidation behaviour of U in the simulated $(U,Ce)O_{2+x}$ MOX fuel with different compositions of Ce, prepared through the ammonia internal gelation route and oxidized in air at 600 °C, using O/M, XRD and XPS analyses in the light of dry storage of MOX and light water reactor spent fuel.

2. Experimental

Various compositions of urania–ceria solid solutions were prepared through the ammonia internal gelation technique. The details of the materials used and the synthesis procedures are discussed elsewhere [35]. The pellets sintered at 1100 °C for 24 h in an atmosphere of $Ar + 2\%$ H_2 were heated in air at 600 °C for 24 h and quenched. The O/M ratio of the oxidized samples was determined by using titrimetric method [32].

The XRD patterns of the sintered and oxidized samples were obtained within the 5 mass% threshold for the detection impurity phases by a Philips X-ray diffractometer (XPERT MPD system, M/s. Philips, The Netherlands) employing filtered Cu Kα radiation.

The photoelectron spectra were taken using a VG ESCALAB MK200X spectrometer with a 150 mm hemispherical analyzer. An Al Kα X-ray source with 20 eV pass energy of the analyzer was used for recording the spectra. The data acquisition and processing were carried out using Eclipse software. The instrument was calibrated with the Au $4f_{7/2}$ peak at 84 eV with 1.6 eV full width at half maximum (FWHM) [36] for the Au film spectrum on Si substrate [37]. The samples for the XPS analysis were prepared by pressing thin pellets of the mixed oxides in indium foil. The foil was attached to a stainless steel stub for mounting on to the *X–Y–Z* translator of the XPS system. Suitable corrections owing to the charging effects were made by monitoring the background In $3d_{5/2}$ signal at 443.8 eV and C 1s signal at 284.6 eV.

3. Results and discussion

The various compositions of the sintered urania–ceria mixed oxides were found to be of cubic fluorite structure upon XRD analyses. The XRD patterns of the air oxidized urania–ceria mixed oxides with varying Ce mole percentage are given in Fig. 1. The XRD pattern of the oxidized product corresponding to the compositions of 8.5, 16.0 and 31.3 mol% Ce ($100 \cdot Ce/(U + Ce)$) was found to be a mixture of orthorhombic and cubic phases. The

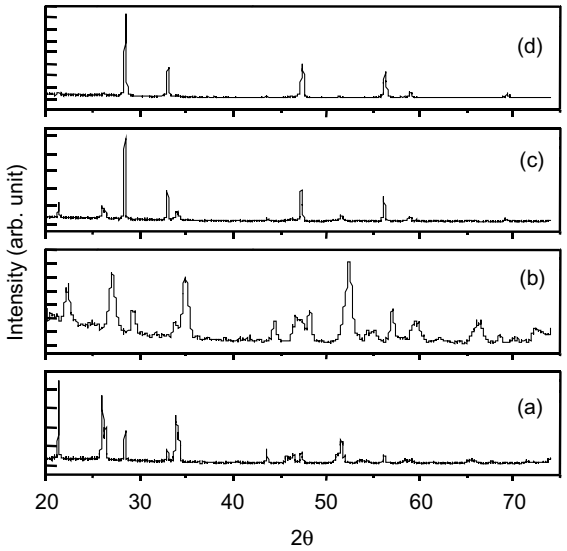

Fig. 1. XRD pattern of the oxidized urania–ceria samples with (a) 8.5, (b) 16.0, (c) 31.3 and (d) 69.0 mol% of Ce ($100 \cdot Ce/(U + Ce)$).

segregation of MO_{2+x} ($M = (U + Ce)$) cubic phase observed during the oxidation of the mixed oxide containing 8.5 mol% Ce is in agreement with the results of Tagawa and Fujino [38] and is in contrast to the results reported by Nawada et al. [32] wherein the limit of the M_3O_8 single-phase region was found to be close to 12 mol% Ce. The phase separation observed in this study can be attributed to the long duration (24 h) of annealing of the sample in air as compared to 8–10 h reported in the earlier study [32]. The oxidation of the mixed oxide with 69 mol% Ce ($100 \cdot Ce/(U + Ce)$) resulted in a single cubic phase (Fig. 1(d)). This indicates that the oxides with a Ce content more than 69 mol% oxidized to a MO_{2+x} single phase. The oxide pellets with 8.5 and 16 mol% Ce were found to crumble during the air oxidation, confirming a phase change with a larger volume of M_3O_8. The M_3O_8 formed has a orthorhombic structure and a lower density (23% less than that of cubic MO_{2+x}) corresponding to a 36% net volume increase [14]. The O/M ratio of the various compositions was determined to calculate the valency of U in the oxidized samples. Results of the O/M and structural analyses of the various compositions are given in Table 1.

A detailed investigation of the oxidation state of U in the oxidized urania–ceria system was carried out using XPS. The oxidation state of U was obtained from the chemical shift of the U $4f_{7/2}$ peak position in the XPS [20]. As the oxidation state decreases from VI to IV, the binding energy corresponding to the peak also decreases. In addition, for the same oxidation state the neighbouring ions cause a change in the binding energy. Since oxygen bonds exist in U(V) and U(VI) oxidation states, which are represented as UO_2^+ and UO_2^{++}, a marginal

Table 1
Results of the O/M and XRD analyses of samples with different cerium contents

100·Ce/(U + Ce) (mol%)	O/M	U valency	Structure analysis		
			2θ (°)	*hkl*[a]	Phases[a]
8.5	2.67	5.46	21.42	002 (o)	o + c
			26.09	310 (o)	
			33.95	312 (o)	
			51.70	430 (o)	
			28.47	111 (c)	
			32.99	200 (c)	
16	2.56	5.33	21.44	002 (o)	o + c
			26.10	310 (o)	
			34.00	312 (o)	
			51.80	430 (o)	
			28.51	111 (c)	
			33.01	200 (c)	
31.3	2.34	4.98	28.45	111 (c)	c + o
			32.96	200 (c)	
			47.31	220 (c)	
			56.15	311 (c)	
			21.42	002 (o)	
			26.10	310 (o)	
69.02	2.13	4.83	28.53	111 (c)	c
			33.05	200 (c)	
			47.41	220 (c)	
			56.25	311 (c)	

[a] o = orthorhombic; c = cubic.

change in the binding energy is observed for the peak corresponding to these oxidation states.

In addition to the peak position, the peak width, which is determined by the FWHM also gives the oxidation state. The FWHM of a peak is related to the lifetime of the excited state, which is a direct consequence of the chemical environment or bonding. Merging of two peaks give rise to a very high value for the FWHM. This is because of multiple oxidation states and the peaks can be resolved by using deconvolution procedures [20].

Another tool used to find the valence-band information and the chemical interaction of a particular ion is the position of the satellite peak. During the expulsion of the core electron by a photon, the valence electron of an ion is either excited to a higher empty orbital or knocked off to the continuum. Owing to this, a peak appears at a few eV higher than the normal binding energy peak in the spectrum and the peak is referred to as satellite peak. In the case of U, the spin–orbit interaction separates the U $4f_{7/2}$ and U $4f_{5/2}$ levels by 10.85 eV and hence the satellites of U $4f_{7/2}$, which generally appear in this energy range are buried in the intense of U $4f_{5/2}$ peak or may appear as shoulder. Hence, in the present study the satellite of the U $4f_{5/2}$ has been taken for the spectral interpretation. During oxidation, the occurrence of valence-band redistribution effects the satellite peak position. The U 4f photoelectron spectra in oxides exhibit a satellite peak of low intensity. Hence, proper identification of the satellite peak in a mixed oxide system is difficult. The characteristic binding energy, FWHM and the satellite peak position corresponding to the different oxidation states of U in pure UO_2 and in some U bearing ternary compounds reported by Bera et al. [20] are given in Table 2. Veal et al. [39] reported that the binding energy for U $4f_{7/2}$ ranges from 379.9 to 380.9 eV and from 380.7 to 381.9 eV, respectively, for UO_2 and UO_3. The FWHM for U(IV) and U(VI) were less than 3 eV. Bera et al. [20] have reported the U $4f_{7/2}$ peak position for U(V) at 380.4 eV with a value of 2.4 eV for FWHM. Pireaux et al. [30] have reported satellites for U(IV) at 5.8, 8.2 and 16 eV higher binding energy than the U 4f photopeak position. In the case of U(IV), the 5.8 and 16 eV satellites of U $4f_{7/2}$ should be clearly seen [30]. In the case of U(VI), the satellites are at 3.7 and 10.6 eV away from the principal peaks. Bera et al. [20] have reported that the satellite peak position of U(IV) is at 6.8 eV higher binding energy than the U $4f_{5/2}$ peak and the corresponding one for U(VI) is at 4.4 eV.

The X-ray photoelectron spectra of U in the air oxidized samples with varying Ce content are given in

Table 2
Photoelectron peak parameters for different uranium chemical states

Oxide	Uranium oxidation state	Peak position of U $4f_{7/2}$ (eV)	FWHM of U $4f_{7/2}$ (eV)	Satellite of U $4f_{5/2}$ (eV)
UO_2	IV	379.9	2.2	6.8
$Sr_2U_3O_{10}$	V	380.4	2.4	8.5
$Rb_2U_4O_{13}$	VI	381.1	2.5	4.4

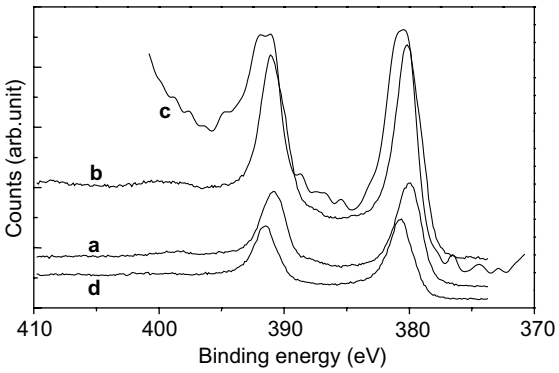

Fig. 2. X-ray photoelectron spectra of uranium in the oxidized samples with (a) 69.0, (b) 31.3, (c) 16.0 and (d) 8.5 mol% of Ce ($100 \cdot Ce/(U + Ce)$).

Fig. 2. The peak positions, FWHM of the U $4f_{7/2}$ peaks and satellite peaks of U $4f_{5/2}$ are summarized in Table 3. The U $4f_{7/2}$ peaks of U in the oxidized samples are found to be higher than 379.9 eV which correspond to U(IV) and are lower than 381 eV corresponding to U(VI).

The $4f_{7/2}$ peaks and their FWHM of the oxidized samples with Ce contents of 16.0, 31.3 and 69.0 mol% are closer to that of U(V) reported by Bera et al. [20] and are less than those reported by Finnie et al. [21]. Hence, it is confirmed that U in these oxides shows an oxidation state close to V. The gradual increase in the binding energies can be attributed to the regular increase in the oxidation states with a decrease in Ce content. This corroborates the XRD and O/M ratio results and it is understood that U in these samples exhibits oxidation states close to the range 4.5 (as in U_4O_9) to 5.3 (as in U_3O_8) which is in agreement with that reported by Nawada et al. [32] who had employed the O/M analysis for the U valency determination in the oxidized urania–ceria system.

In the case of $U_{0.915}Ce_{0.085}O_{2.67}$, the U $4f_{7/2}$ peak appeared at 380.9 eV of which the value is less than that of U(VI) in UO_3 [38] and more than that of U(V). Hence, U in this oxide exhibits an oxidation state higher than that in U_3O_8 and lower than the one in UO_3, which also supports the O/M result. The higher valency of U in this oxide than that in U_3O_8 may be due to the incorporation of CeO_2 into the U_3O_8 phase.

The position of the satellite peak of U $4f_{5/2}$ peaks is yet another tool to support the oxidation state of U in the mixed oxides. In the present study satellite peaks are found to be very weak and in some cases they were indistinguishable. The oxide with 8.5 mol% Ce shows a satellite peak around 5 eV which is close to the one found in UO_3 and in the other oxides it is around 8 eV confirming the presence of oxidation states very close to (VI) and (V) in the mixed oxides.

The 3d photoelectron spectra of Ce in the oxidized samples are found to be in good agreement with that of pure CeO_2 recorded under the same conditions. This shows that Ce in the oxidized samples exists as Ce(IV). The Ce 3d spectrum consists of six peaks. The multiple peak result from a final state shake-down which places a different occupation in the O 2p and Ce 4f valence orbitals. The 3d spectra of Ce in pure CeO_2 as well as in the mixed oxides with 8.5 and 69 mol% of Ce are given in Fig. 3. The O 1s spectrum of oxygen gives a binding energy peak around 530 eV, which is characteristic of the metal oxides.

Table 3
XPS results of uranium in the oxidized samples with different cerium contents

$100 \cdot Ce/(U + Ce)$ (mol%)	Peak position (eV)		FWHM of U $4f_{7/2}$ (eV)	Satellite of U $4f_{5/2}$ (eV)
	U $4f_{7/2}$	U $4f_{5/2}$		
69.0	380.1	391.1	2.3	8
31.3	380.3	391.1	2.4	8.3
16.0	380.4	391.2	2.4	–
8.5	380.9	391.8	2.5	5

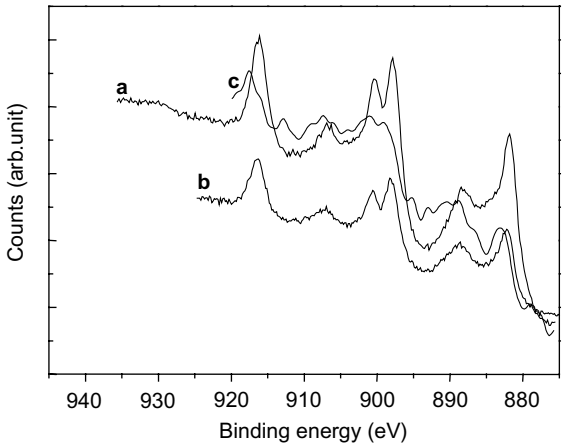

Fig. 3. X-ray photoelectron spectra of cerium in the oxidized samples with (a) 100, (b) 69 and (c) 8.5 mol% of Ce (100·Ce/(U + Ce)).

4. Conclusion

The air oxidation behaviour at 600 °C of urania–ceria solid solutions prepared through the internal gelation route was investigated by means of XRD, O/M and XPS analyses. The XRD analysis revealed that the oxidation of the samples containing less than 70 mol% Ce ends up in a mixture of orthorhombic M_3O_8 and cubic MO_{2+x} phases and the solid solution with Ce contents above 70 mol% yields single-phase cubic MO_{2+x}. The valencies of U in the oxidized samples were determined using O/M and XPS analyses. It has been observed that an increase in Ce content resists the formation of U_3O_8 during the oxidation of urania–ceria solid solutions.

Acknowledgements

The authors are grateful to Dr S. Bera, WSCL, BARC (F), Kalpakkam for recording the XPS and to Shri G. Paneerselvam, FChD, IGCAR, Kalpakkam for recording the XRD patterns. The authors are also thankful to Dr C. Mallika, TKD, MCG, IGCAR, Kalpakkam and to Shri K.V. Mahudeeswaran, Chief superintendent, Kalpakkam reprocessing plant, BARC (F), Kalpakkam for their encouragement. This work constitutes a part of the PhD thesis of K. Suresh Kumar to be submitted to the University of Madras, India.

References

[1] INFCE Working Group 5, IAEA Report, STI/PUB 534, 1980.
[2] C.K. Gupta, Materials in Nuclear Energy Applications – I, CRC, Florida, 1989.
[3] S. Aronson, R.B. Roof Jr., J. Belle, J. Chem. Phys. 27 (1957) 137.
[4] M.J. Bannister, J. Nucl. Mater. 26 (1968) 174.
[5] J. Belle, in: Uranium Dioxide: Properties and Nuclear Applications, Naval Reactors Handbook, Division of Reactor Development, USAEC, 1961.
[6] P.E. Blackburn, J. Weissbart, E.A. Gulbransen, J. Phys. Chem. 62 (1958) 902.
[7] K.T. Harrison, C. Padgett, K.T. Scott, J. Nucl. Mater. 23 (1967) 121.
[8] H.R. Hoekstra, A. Santoro, S. Siegel, J. Inorg. Nucl. Chem. 18 (1961) 166.
[9] P. Taylor, D.D. Wood, A.M. Duclos, J. Nucl. Mater. 189 (1992) 116.
[10] S.R. Teixeira, K. Imakuma, J. Nucl. Mater. 178 (1991) 33.
[11] L.E. Thomas, R.E. Einziger, Mater. Charact. 28 (1992) 149.
[12] L.E. Thomas, O.D. Slagle, R.E. Einziger, J. Nucl. Mater. 184 (1991) 117.
[13] K.M. Wasywich, W.H. Hocking, D.W. Shoesmith, P. Taylor, Nucl. Technol. 104 (1993) 309.
[14] R.J. McEachern, P. Taylor, J. Nucl. Mater. 254 (1998) 87.
[15] T. Smith, Atomic International Report, NAA-SR-4677, 1960.
[16] H. Landspersky, M. Vobori, J. Inorg. Nucl. Chem. 29 (1966) 153.
[17] L.E. Thomas, R.E. Einziger, H.C. Buchanan, J. Nucl. Mater. 201 (1993) 310.
[18] J.W. Choi, R.J. McEachern, P. Taylor, D.D. Wood, J. Nucl. Mater. 230 (1996) 250.
[19] S. Sunder, N.H. Miller, J. Nucl. Mater. 231 (1996) 121.
[20] S. Bera, S.K. Sali, S. Sampath, S.V. Narasimhan, V. Venugopal, J. Nucl. Mater. 255 (1998) 26.
[21] K.S. Finnie, Z. Zhang, E.R. Vance, M.L. Carter, J. Nucl. Mater. 317 (2003) 46.
[22] P.A. Tampest, P.M. Tucker, J.W. Tyler, J. Nucl. Mater. 151 (1988) 251.
[23] R.J. McEachern, S. Sunder, P. Taylor, D.C. Doern, N.H. Miller, D.D. Wood, J. Nucl. Mater. 255 (1998) 234.
[24] W.Y. Howng, R.J. Thorn, Chem. Phys. Lett. 62 (1979) 57.
[25] D. Chadwick, Chem. Phys. Lett. 21 (1973) 291.
[26] S.V. Berghe, F. Miserque, T. Gouder, B. Gaudreau, M. Verwerft, J. Nucl. Mater. 294 (2001) 168.
[27] S. Anthonysamy, G. Paneerselvam, S. Bera, S.V. Narasimhan, P.R. Vasudeva Rao, J. Nucl. Mater. 281 (2000) 15.
[28] S. Sunder, G.D. Boyer, N.H. Miller, J. Nucl. Mater. 175 (1990) 163.
[29] S. Sunder, N.H. Miller, J. Nucl. Mater. 279 (2000) 118.
[30] J.J. Pireaux, J. Riga, E. Thibaut, C.T. Noel, R. Caudano, J.J. Verbist, Chem. Phys. 22 (1977) 113.
[31] C. Keller, C.K. Jorgensen, Chem. Phys. Lett. 32 (1975) 397.
[32] H.P. Nawada, P. Sriramamurti, K.V. Govindankutty, S. Rajagopalan, R.B. Yadav, P.R. Vasudeva Rao, C.K. Mathews, J. Nucl. Mater. 139 (1986) 19.
[33] S.V. Chavan, A.K. Tyagi, Thermochim. Acta 390 (2002) 79.
[34] P. Martin, M. Ripert, T. Petit, T. Reich, C. Hennig, F. D'Acapito, J.L. Hazemann, O. Proux, J. Nucl. Mater. 312 (2003) 103.

[35] K.S. Kumar, H.P. Nawada, N.P. Bhat, J. Nucl. Mater. 321 (2003) 263.
[36] D.K. Sarkar, S. Bera, S. Dhara, K.G.M. Nair, S.V. Narasimhan, S. Choudhary, Appl. Surf. Sci. 120 (1997) 159.
[37] C.J. Powell, Surf. Interface Anal. 23 (1995) 121.
[38] H. Tagawa, T. Fujino, Bull. Chem. Soc. 54 (1981) 138.
[39] B.W. Veal, D.J. Lam, H. Diamond, H.R. Hoekstra, Phys. Rev. B 15 (1977) 2929.